Research Square

Preprints are preliminary reports that have not undergone peer review.
They should not be considered conclusive, used to inform clinical practice,
or referenced by the media as validated information.

A context-dependent glucocorticoid receptor-SCARA5 axis coupled to ferritin/iron handling in osteoporotic bone marrow stromal cell fate: transcriptomic reanalysis and regulatory nomination

Beiji Lu

drlubeiji@outlook.com

Xuzhou Central Hospital, Affiliated Hospital of Southeast University; Xuzhou Medical University Clinical College https://orcid.org/0009-0004-9876-1883

Research Article

Keywords: SCARA5, glucocorticoid receptor, NR3C1, osteoporosis, bone marrow stromal cells, ferritin, iron handling, transcriptomic reanalysis

Posted Date: October 7th, 2026

DOI: https://doi.org/10.21203/rs.3.rs-11273765/v1

License: This work is licensed under a Creative Commons Attribution 4.0 International License.
Read Full License

Additional Declarations: The authors declare no competing interests.

A context-dependent glucocorticoid receptor–SCARA5 axis coupled to ferritin/iron handling in osteoporotic bone marrow stromal cell fate: transcriptomic reanalysis and regulatory nomination

Running title: GR–SCARA5 receptor-output axis in BMSC fate

Beiji Lu

Department of Orthopedics, Xuzhou Central Hospital, Affiliated Hospital of Southeast University, No. 99 Jiefang Road, Xuzhou, Jiangsu 221000, China; Xuzhou Medical University Clinical College, Xuzhou, Jiangsu 221000, China

* Corresponding author. Email: 753007215@qq.com

Abstract

Bone marrow stromal cell (BMSC) fate is central to the remodelling imbalance that accompanies osteoporosis, but the upstream regulators linking glucocorticoid signalling to the osteogenic–adipogenic fate balance remain incompletely defined. Here we combine transcriptomic reanalysis, promoter and public regulatory evidence, and receptor-output correlation to characterise the relationship between the glucocorticoid receptor (GR/NR3C1) and SCARA5 in osteoporosis-relevant BMSC fate. In human mesenchymal stromal cells (hMSCs) undergoing osteogenic induction, SCARA5 was among the most strongly regulated transcripts: it fell 7.7-fold (log2FC = −2.94, adjusted P = 4.7e-169) under Pyk2 inhibition and ranked in the top 10 of 15,410 tested genes by adjusted P value, while the canonical osteogenic marker ALPL rose (log2FC = +2.19, adjusted P = 4.6e-185). Because dexamethasone was present in both arms of this dataset and NR3C1 transcript was unchanged (log2FC = −0.13), the dataset identifies SCARA5 as a strongly regulated effector in a glucocorticoid-containing osteogenic context but cannot by itself attribute that regulation to GR. NR3C1 mRNA was not a readout of GR activity: in an independent glucocorticoid-treated primary BMSC dataset, six canonical GR target genes were induced in all four donors while NR3C1 mRNA fell (log2FC = −0.65,

adjusted P = 1.6e-21). A candidate glucocorticoid response element is present in the SCARA5 proximal promoter, and public ENCODE GR ChIP-seq nominates the locus as GR-responsive in non-BMSC cell lines; however, GR activation alone did not induce SCARA5 in undifferentiated primary BMSCs. Receptor-output correlation identified ferritin/iron handling as the strongest SCARA5-linked module (mean |r| = 0.909, 8 of 10 genes significant), with FTH1 (r = +0.9985), SLC40A1 (r = +0.9895) and FTL (r = +0.9850) as positive anchors and the osteogenic markers COL1A1 (r = −0.9997) and ALPL (r = −0.9989) inversely correlated. Together these findings position GR–SCARA5 as a context-dependent, receptor-output-coupled axis in osteoporotic marrow remodelling, and define a regulatory nomination whose causal validation requires functional perturbation.

Introduction

Osteoporosis reflects a failure of skeletal remodelling in which bone formation, bone resorption, and bone marrow stromal cell (BMSC) fate are no longer balanced. BMSCs are central to this process because they supply osteogenic progenitors while retaining the capacity to enter adipogenic programmes; disruption of the osteogenic–adipogenic fate balance in the stromal compartment contributes to marrow adiposity and impaired bone formation in osteoporosis-relevant settings.

SCARA5, a class A scavenger receptor, has emerged as a stromal effector gene connected to BMSC differentiation and to marrow remodelling. The stronger biological question is not whether SCARA5 changes, but which upstream regulator connects it to osteoporosis-relevant cellular and pharmacological context.

NR3C1 encodes the glucocorticoid receptor (GR), a transcription factor with well-established relevance to endocrine signalling and to glucocorticoid-associated skeletal effects. The hypothesis examined here is that GR activity is coupled to SCARA5 expression, and that SCARA5 in turn couples to a receptor-output programme that biases the osteogenic–adipogenic balance of BMSCs. Three lines of evidence motivate this. A glucocorticoid response element is present in the SCARA5 proximal promoter. Prior work links SCARA5 to mesenchymal stem cell adipogenic commitment (PMID 29093466). And a receptor-output correlation analysis shows that SCARA5 abundance tracks

positively with ferritin and iron-handling transcripts and inversely with canonical osteogenic markers.

We show that this relationship is genuine but conditional. Public transcriptomic reanalysis places SCARA5 among the most strongly regulated effectors in a glucocorticoid-containing osteogenic context, and receptor-output correlation couples it to ferritin/iron handling. Public promoter and regulatory evidence nominates NR3C1/GR as the upstream candidate. Yet GR activation on its own, applied to undifferentiated primary BMSCs, does not switch SCARA5 on. The axis is therefore best described as requiring GR activity together with a permissive differentiation context; direct functional validation of GR causality is ongoing and will be reported separately.

Results

SCARA5 is among the most strongly regulated genes in Pyk2-inhibited hMSCs undergoing osteogenic induction

We reanalysed the GSE266328 hMSC transcriptomic dataset. Human bone marrow-derived mesenchymal cells (Lonza) were cultured in osteogenic differentiation medium containing ascorbic acid, β-glycerophosphate and dexamethasone, and exposed to the Pyk2 inhibitor PF-4618433 (50 nM) or vehicle DMSO for 4 days (n = 3 per group; 58 bp paired-end, reverse-stranded libraries). Counts were quantified against Ensembl GRCh38, filtered to genes with at least 10 reads across all samples (62,754 → 20,603), and tested with DESeq2 median-of-ratios normalisation (size factors 0.919–1.181).

SCARA5 normalised counts fell from 1,127–1,145 in vehicle-treated cells to 144–154 under Pyk2 inhibition, a 7.67-fold reduction (log2FC = −2.94, adjusted P = 4.7e-169). Among the 15,410 genes that passed independent filtering, SCARA5 ranked 10th by adjusted P value and 17th by absolute fold change, placing it in the top 0.065% of the tested transcriptome and making it the only scavenger receptor family member in that group. The direction is consistent with the primary report of this dataset, in which SCARA5 was among the most strongly downregulated transcripts and was independently confirmed by qPCR (PMID 39578816). In the same comparison the canonical osteogenic marker ALPL rose 4.6-fold (log2FC = +2.19, adjusted P = 4.6e-185), and pathway enrichment separated cleanly by direction: genes upregulated under Pyk2 inhibition were enriched for muscle structure development and smooth muscle contraction,

while downregulated genes were enriched for humoral immune response and complement cascade (Fig. 1).

Two boundaries follow from the design of this dataset. First, dexamethasone was present in the medium of both arms, so glucocorticoid receptor activation was constant and the only experimental variable was Pyk2 inhibition. This dataset therefore identifies SCARA5 as a strongly regulated effector in a glucocorticoid-containing osteogenic context, but it cannot by itself attribute that regulation to GR. Second, the analysis rests on a single dataset with n = 3 per group; no cross-dataset transcriptomic replication of the Pyk2-inhibition comparison is available.

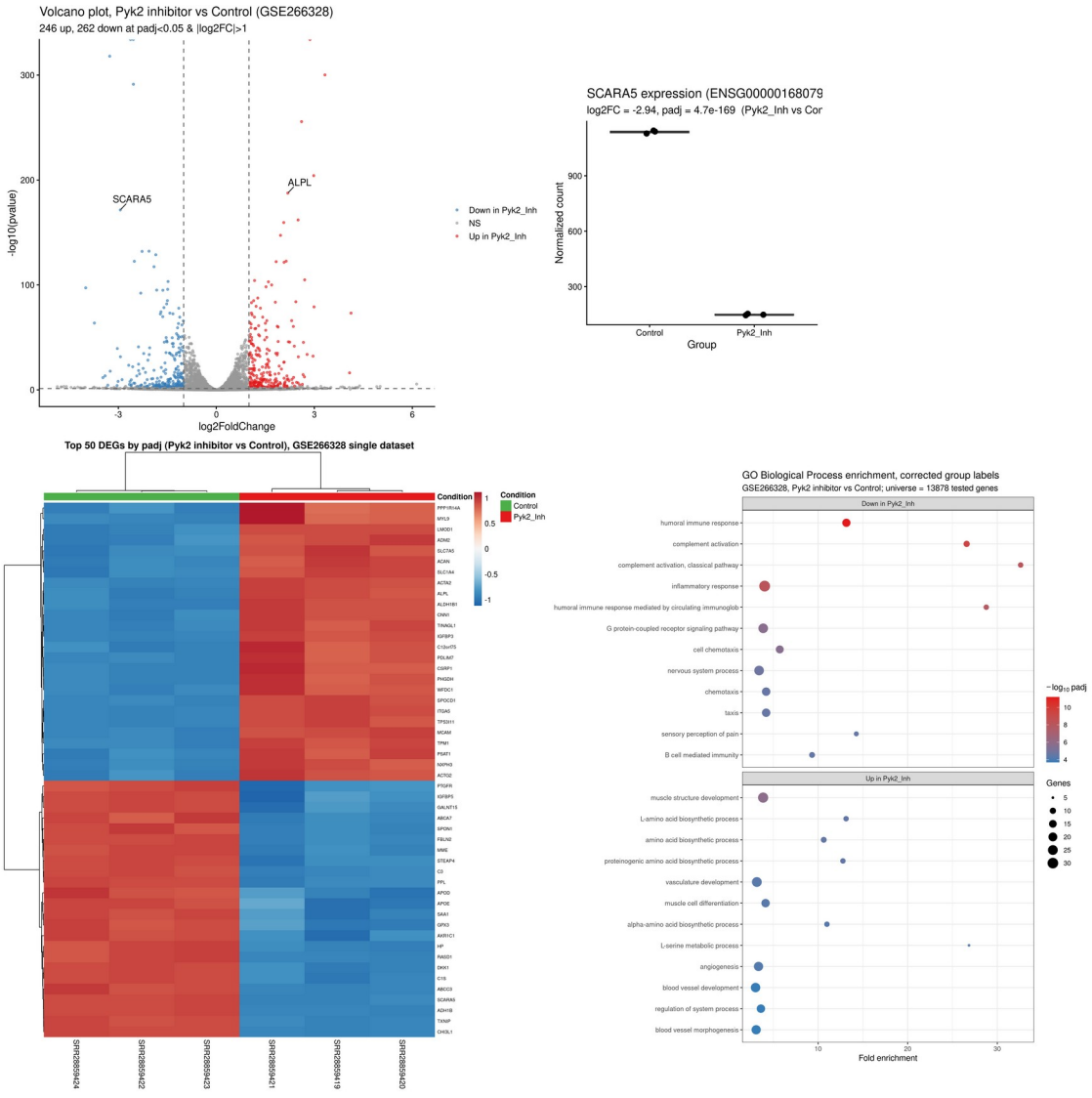


Figure 1

A GRE-linked promoter and public regulatory maps nominate NR3C1/GR upstream of SCARA5, and NR3C1 mRNA is not a readout of GR activity

To identify a candidate upstream regulator, the SCARA5 proximal promoter was scanned with JASPAR GR/NR3C1 position weight matrices, which identified a candidate glucocorticoid response element (Fig. 2). This is consistent with prior work linking SCARA5 transcription to glucocorticoid signalling and to MSC adipogenic commitment (PMID 29093466). Public ENCODE NR3C1/GR ChIP-seq shows recurrent GR occupancy at the SCARA5 locus across 32 released experiments in five non-BMSC cell lines (A549, K562, HepG2, Ishikawa, WTC11; Methods). These peaks are distal rather than promoter-proximal, lying 52.6–119.8 kb from the transcription start site within the gene body, so they nominate the locus as GR-responsive without corroborating the proximal-promoter element identified above. The strongest peak overlaps accessible enhancer-like chromatin in H1-derived mesenchymal stem cell DNase and IMR-90 ATAC/DNase data, with osteoblast DNase and UCSC cCRE annotation as additional context; these are accessibility datasets and are not themselves occupancy evidence. Taken together the public data nominate SCARA5 as a GR-linked regulatory locus in a mesenchymal-accessible chromatin context. They are not evidence of direct GR binding in BMSCs, and the absence of any bone-marrow mesenchymal, osteoblastic or fibroblastic biosample among the 32 experiments is itself a limitation of this layer.

NR3C1 mRNA was unchanged in the Pyk2-inhibition comparison (log2FC = −0.13, adjusted P = 0.31). Rather than treating this as a gap, we tested directly whether NR3C1 transcript level tracks GR activity, using an independent RNA-seq dataset of primary human bone marrow MSCs from four donors treated with the glucocorticoid agonist triamcinolone acetonide (10 nM, 24 h) against paired vehicle controls (GSE240387; analysed as `~ donor + treatment`). Six canonical GR target genes were induced in every donor without exception: FKBP5 (log2FC = +4.41), PER1 (+3.30), TSC22D3 (+2.71), KLF9 (+2.19), DUSP1 (+1.60) and SGK1 (+0.94), each significant and concordant in 4/4 donors. In the same samples NR3C1 mRNA fell (log2FC = −0.65, adjusted P = 1.6e-21, 4/4 donors), consistent with established ligand-dependent autologous downregulation of the receptor transcript.

NR3C1 mRNA level therefore cannot serve as an indicator of GR pathway activity in this system: GR activation sufficient to induce FKBP5 more than 20-

fold was accompanied by a decrease in NR3C1 transcript. GR involvement in the SCARA5 axis was consequently pursued through promoter and literature anchoring, public regulatory nomination, and the sufficiency test described below, rather than through transcript abundance.

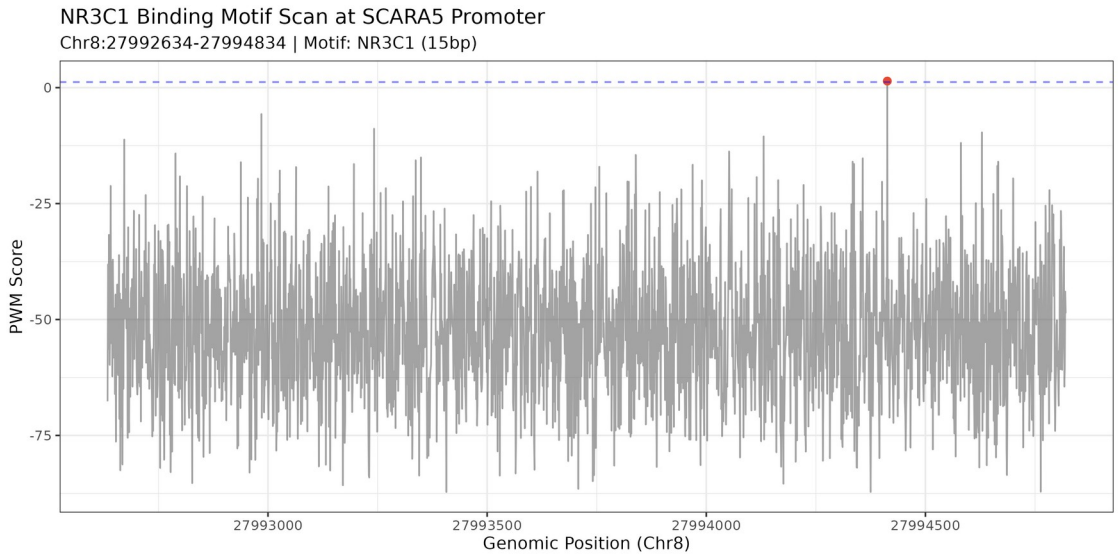


Figure 2

Receptor-output scoring links SCARA5 to ferritin/iron handling

To characterise the functional neighbourhood of SCARA5, we correlated SCARA5 expression against curated candidate modules for ferritin/iron handling, lipoprotein/lipid handling, adhesion/ERK signalling, and osteogenic/adipogenic fate, using log2-transformed DESeq2-normalised counts from the prefiltered GSE266328 matrix (Fig. 3).

Ferritin/iron handling was the strongest module (mean $|r| = 0.909$; 8 of 10 genes significant at $p < 0.05$, which with $n = 6$ requires $|r| > 0.811$). The positive anchors were FTH1 ($r = +0.9985$), SLC40A1 ($r = +0.9895$), FTL ($r = +0.9850$), HMOX1 ($r = +0.9818$) and SLC11A2 ($r = +0.9749$); three members correlated negatively — SLC7A11 ($r = −0.8805$), TFRC ($r = −0.8652$) and ACSL4 ($r = −0.8304$) — so the directional mean r is +0.393 and the module is best described as strong but not uniformly signed. Within the osteogenic/adipogenic module, the canonical osteogenic markers COL1A1 ($r = −0.9997$) and ALPL ($r = −0.9989$) were inversely correlated with SCARA5, so high SCARA5 tracks with suppression of osteogenic matrix and mineralisation transcripts. The lipoprotein/lipid module (mean $|r| = 0.791$) and the adhesion/ERK module (mean $|r| = 0.773$) were mixed

in direction and are reported as receptor and cargo remodelling context rather than as evidence of net pathway activation.

Read together with the direction of the Pyk2-inhibition comparison, the iron module describes a coherent pattern: SCARA5 fell alongside the ferritin storage and export machinery (FTH1 log2FC = −0.72, FTL = −1.09, SLC40A1 = −1.09, HMOX1 = −0.94) while the transferrin receptor TFRC rose (+0.25). Reduced ferritin storage transcripts with increased TFRC is the classical IRP/IRE response to low intracellular iron, and it is consistent with SCARA5's established role as a ferritin receptor mediating non-transferrin-bound iron uptake (PMID 19154717) — that is, with SCARA5 positioned upstream of the iron-handling output rather than downstream of it.

Three limits apply. Iron content, ferritin uptake and IRP activity were not measured here, so the above is a directional inference from co-expression and prior receptor biology, not a demonstration. SLC7A11 (log2FC = +0.55) and ACSL4 (+0.26) moved in opposite directions with respect to ferroptosis susceptibility, so no ferroptosis claim is made. And the osteogenic arm of the fate module is thinner than its gene list suggests: SP7 (Osterix) and BGLAP (osteocalcin) were undetectable in this dataset (2 and 4 reads respectively across all six samples) and were removed by count filtering, leaving RUNX2, ALPL and COL1A1 as the only measurable osteogenic members.

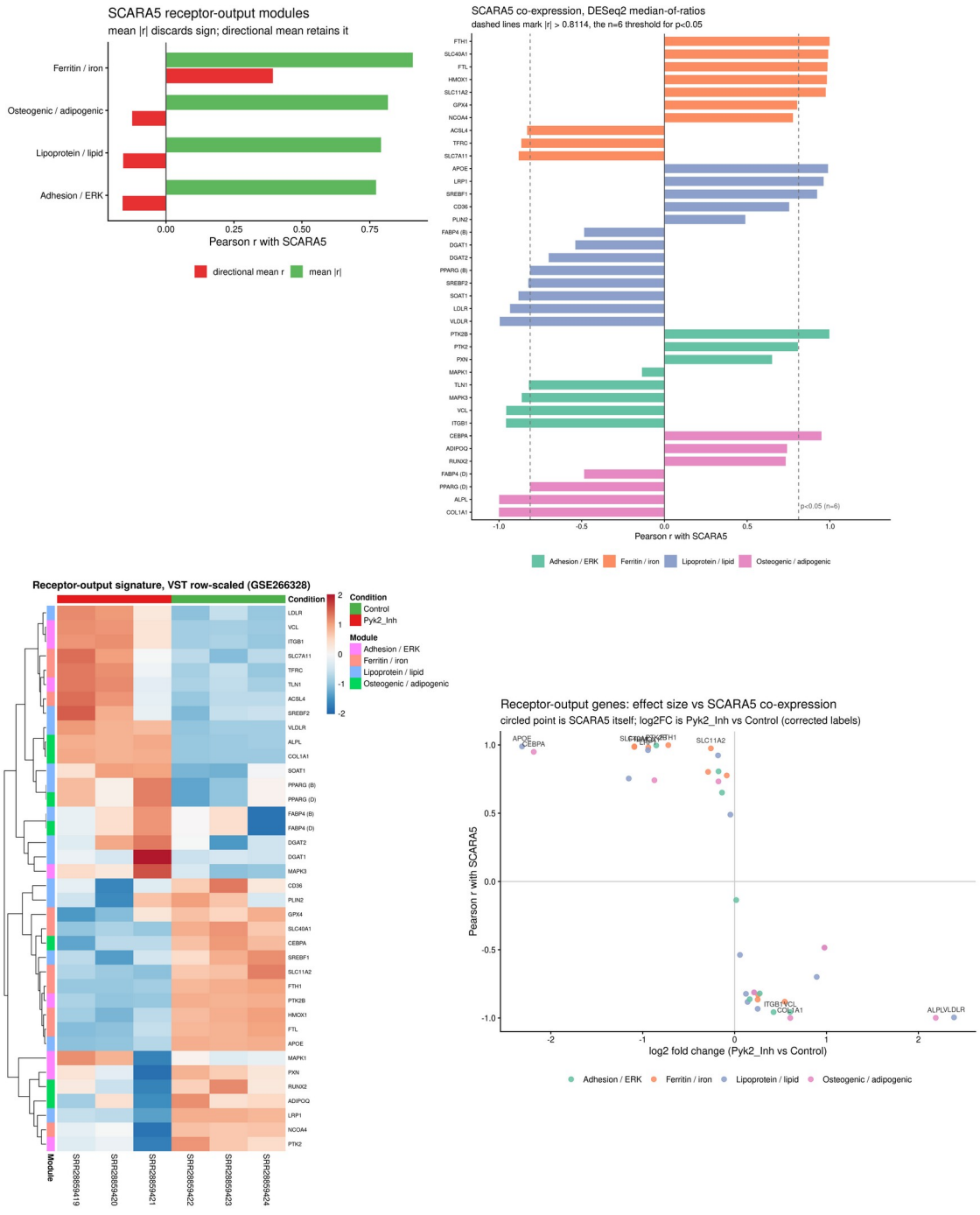


Figure 3

Glucocorticoid receptor activation alone does not induce SCARA5 in undifferentiated BMSCs

Because the primary dataset could not separate GR activation from Pyk2 inhibition, we asked directly whether GR activation is sufficient to induce

SCARA5, using the paired glucocorticoid dataset described above (GSE240387; primary human bone marrow MSCs, four donors, triamcinolone acetonide 10 nM for 24 h in complete medium without differentiation induction).

The treatment was unambiguously effective, inducing all six canonical GR targets in all four donors. SCARA5, however, was not expressed: mean normalised count 1.9 across the eight libraries, with two of four donors at exactly zero in both arms, against 212–441 (vehicle) and 5,034–7,324 (agonist) for FKBP5 in the same samples. SCARA5 was removed by independent filtering and no adjusted P value could be assigned. We report this as a negative result. It is not evidence against the axis, because the culture conditions are not comparable to the primary dataset — 24 h in complete medium without induction versus 4 days in dexamethasone-containing osteogenic medium — but it does place a boundary on the claim: GR activation on its own, in undifferentiated BMSCs, does not switch SCARA5 on.

A published hMSC differentiation time course is consistent with the same boundary. In hMSCs induced toward adipogenic or osteogenic fate (GSE80614), where dexamethasone is a component of both induction media, SCARA5 remained at the detection floor for the first 12 h in both arms and rose only from day 1 onward, and only in the adipogenic arm (log2 signal 6.9 → 9.2 by day 2, versus 6.9 → 7.2 in the osteogenic arm across 4 days). The most precise statement the present data support is that GR activity is necessary but not sufficient for SCARA5 expression, and that a permissive differentiation context is additionally required. Accordingly, we describe the SCARA5 promoter GRE as a regulatory nomination rather than as a demonstrated direct induction mechanism.

Discussion

This manuscript supports a focused regulatory nomination rather than a causal mechanism. The most defensible claims are that SCARA5 is a strongly regulated effector in a glucocorticoid-containing osteogenic context, that it is coupled to a ferritin/iron-handling output and inversely to osteogenic matrix transcripts, and that GR is nominated as the upstream regulator whose activity is necessary but not sufficient for SCARA5 expression.

The argument rests on three layers with deliberately unequal weight. Public transcriptomic reanalysis nominates SCARA5 as one of the most strongly

regulated effectors in an hMSC perturbation relevant to stromal differentiation, and characterises its co-expression neighbourhood. Promoter GRE evidence, prior MSC literature and public ENCODE regulatory maps nominate NR3C1/GR as the upstream candidate. The conditional boundary — that GR activation alone is insufficient — is established by a paired glucocorticoid dataset in primary BMSCs and by a published differentiation time course.

A division of labour follows from the design of the primary dataset and deserves to be stated plainly. In GSE266328 both arms were cultured in dexamethasone-containing osteogenic medium for four days, so GR was ligand-activated on both sides and the experimental variable was Pyk2 inhibition. The dataset can therefore establish that SCARA5 is strongly regulated in a glucocorticoid-containing osteogenic context, and that its regulation is anticorrelated with osteogenic markers, but it cannot attribute that regulation to GR. Any reading in which the transcriptome demonstrates GR-driven SCARA5 induction over-interprets the design. For this reason the causality of the axis is assigned to functional perturbation, which is ongoing and will be reported separately.

An unexpectedly informative negative concerns NR3C1 transcript abundance. NR3C1 mRNA did not change under Pyk2 inhibition, and in the paired glucocorticoid dataset it fell while GR output rose sharply. Receptor transcript level is therefore not a proxy for receptor activity in BMSCs, and the absence of NR3C1 mRNA change in the primary dataset carries no evidential weight either for or against the axis. This negative points to where a regulated quantity would have to reside — post-translationally, on receptor activity rather than receptor abundance — and frames the appropriate design for functional validation.

The ferritin/iron arm is the strongest mechanistic signal in the co-expression analysis, and its corrected direction is internally coherent: SCARA5 falls together with ferritin storage and export transcripts while transferrin receptor rises, which is the canonical IRP/IRE signature of reduced intracellular iron and is consistent with SCARA5 acting as a ferritin receptor upstream of that output. Iron content, ferritin uptake and IRP activity were not measured, so this is a directional inference from co-expression and prior receptor biology rather than a demonstration, and it is a primary target for future validation. Within the same module SLC7A11 and ACSL4 moved in opposite directions with respect to ferroptosis susceptibility, so no ferroptosis interpretation is offered.

Several limitations should be stated explicitly. The bioinformatics rests on a single dataset with n = 3 per group; with six samples, a Pearson correlation requires $|r| > 0.811$ to reach $p < 0.05$, so near-unity correlation coefficients are expected rather than remarkable, and the high proportion of significant module members should be read in that light. Module-level mean $|r|$ is reported alongside the directional mean because the absolute value discards sign: the ferritin/iron module contains three negatively correlated members and is strong but not uniformly signed. No cross-dataset transcriptomic replication of the Pyk2-inhibition comparison exists; three external candidates were examined and none was usable (GSE56814 profiles blood monocytes, GSE32530 is a breast-cancer SNP copy-number series rather than an expression dataset, and E-MTAB-9493 uses amnion rather than bone-marrow mesenchymal cells). Human genetic causality evidence from Mendelian randomisation, colocalisation or scPAGWAS is not included; this boundary is intentional. Two provenance limitations affect the receptor-output analysis specifically: an earlier correlation table was computed on log2(CPM+1) rather than on DESeq2 median-of-ratios normalisation, which inflated two module members across the n = 6 significance threshold; the values reported here are recomputed on median-of-ratios counts and the affected members are reported as non-significant. Two genes, FABP4 and PPARG, are biologically members of both the lipoprotein/lipid and the osteogenic/adipogenic fate modules and are reported in both, with the double assignment made explicit in the figure.

Methods

Primary transcriptomic dataset and reanalysis

Public hMSC RNA-seq data were obtained from GEO accession GSE266328 (BioProject PRJNA1106770; runs SRR28859419–SRR28859424). Human bone marrow-derived mesenchymal cells (Lonza) were cultured to confluence and then in osteogenic differentiation medium (Lonza BulletKit) containing ascorbic acid, β-glycerophosphate and dexamethasone, with the Pyk2 inhibitor PF-4618433 at 50 nM or an equivalent percentage of DMSO, for 4 days (n = 3 per group). Libraries were 58 bp paired-end on NovaSeq 6000 and are reverse-stranded (library type ISR, confirmed by automatic inference in all six libraries).

Run-to-sample assignment was taken from the ENA record for PRJNA1106770 and cross-checked against GEO sample titles: SRR28859419/420/421 correspond

to PF4618433-3/-2/-1 (GSM8245000/8244999/8244998) and SRR28859422/423/424 to Control-3/-2/-1 (GSM8244997/8244996/8244995).

The gene-level count matrix derives from a STAR alignment of these runs against Ensembl GRCh38 with HTSeq v2.0.2 quantification (matching the authors' pipeline); genes with fewer than 10 reads summed across all samples were removed (62,754 → 20,603) before differential testing with DESeq2 (median-of-ratios normalisation; size factors 0.919–1.181; Wald test; Benjamini–Hochberg correction). Independent filtering left 15,410 genes with an adjusted P value. Analyses were run under R 4.6.0 with DESeq2 1.52.0. As an independent quantification check, the same six runs were quantified with salmon 2.0.1 and summarised to gene level with tximport before the identical DESeq2 model; effect sizes agreed to within 0.10 log2 units and in direction for all diagnostic genes examined (SCARA5, ALPL, FTH1, FTL, SLC40A1, PTK2B, COL1A1, NR3C1).

Receptor-output correlation analysis

Pearson correlations were computed between log2(DESeq2-normalised count + 1) values for SCARA5 and for each member of four curated candidate modules (ferritin/iron handling, lipoprotein/lipid handling, adhesion/ERK signalling, osteogenic/adipogenic fate), using the prefiltered matrix. Two genes, FABP4 and PPARG, are members of two modules by design and are reported in both. With $n = 6$, $p < 0.05$ corresponds to $|r| > 0.811$; this threshold is drawn explicitly on the figure. Module summaries report both mean $|r|$ and the directional mean r. Genes failing the count filter (LPL, SP7, BGLAP) are excluded and identified in the source table.

Enrichment analysis

Differentially expressed genes (adjusted $P < 0.05$ and $|\log2FC| > 1$) were mapped to Entrez identifiers and tested for over-representation against GO Biological Process, GO Molecular Function and Reactome gene sets using a hypergeometric test with Benjamini–Hochberg correction. The background universe was restricted to genes that entered differential testing and carried an Entrez identifier ($n = 13,878$), rather than to all annotated genes. Gene sets with fewer than 10 or more than 500 members within the universe, and terms with fewer than three overlapping genes, were excluded.

External glucocorticoid dataset

Paired RNA-seq data for primary human bone marrow MSCs treated with triamcinolone acetonide were obtained from GSE240387 (BioProject PRJNA1003481; eight runs, four donors, each with agonist and vehicle). Cells were exposed to triamcinolone acetonide 10 nM or complete DMEM alone for 24 h, without differentiation induction; libraries were 58 bp paired-end and reverse-stranded. The associated publication reports GRCm38 in its Methods, inconsistent with the deposited record, which specifies GRCh38 in both the assembly field and the alignment description and carries 125,406 human Ensembl gene identifiers; analysis here used GRCh38 throughout.

FASTQ files were verified on acquisition against the ENA-reported byte size and MD5 for every file, checked for archive integrity, and independently re-hashed with SHA-256 after transfer before any computation. Quantification used salmon 2.0.1 against a decoy-aware Ensembl GRCh38 index, summarised with tximport, and tested with DESeq2 using the paired design `~ donor + treatment` (three residual degrees of freedom). Mapping rates were 99.0–99.4%. Genes with fewer than 10 reads across all samples were removed (62,269 → 20,791). Detectability for SCARA5 was defined in advance as baseMean $\geqslant$ 10.

Reference-gene stability audit

Because quantitative PCR is conventionally normalised to GAPDH and western blots to β-actin, sixteen commonly used reference genes were examined in both public datasets. Stability was classified in advance as $|\log2FC| < 0.20$ with adjusted $P > 0.05$ and baseMean $\geqslant$ 500. Under glucocorticoid perturbation (GSE240387), GAPDH was stable (log2FC = −0.07, adjusted P = 0.22) whereas ACTB was not (log2FC = +0.32, adjusted P = 1.5e-08); RPL13A, B2M and EEF1A1 were stable. Under Pyk2 inhibition (GSE266328), both ACTB (log2FC = +0.56) and TUBB (+0.46) were strongly regulated, consistent with cytoskeletal remodelling downstream of a focal adhesion kinase, and GAPDH was marginal (+0.18, adjusted P = 0.016).

Promoter motif and regulatory nomination

The SCARA5 proximal promoter was scanned for GR/NR3C1 response elements using JASPAR position weight matrices, identifying a candidate glucocorticoid response element. Public ENCODE NR3C1/GR ChIP-seq was surveyed for occupancy at the SCARA5 locus. As of the analysis date, ENCODE holds 32

released NR3C1 TF ChIP-seq experiments distributed across A549 (24), K562 (3), HepG2 (2), Ishikawa (2) and WTC11 (1); none is in a bone-marrow mesenchymal, osteoblastic or fibroblastic biosample. Open-chromatin context was taken from H1-derived MSC DNase, IMR-90 ATAC/DNase, osteoblast DNase and UCSC cCRE annotation; these accessibility datasets are distinct from the ChIP experiments and are not evidence of receptor occupancy. All public data here are used as regulatory nomination in non-BMSC contexts and are not evidence of GR binding in BMSCs.

Data and code availability

Analysis scripts for every value reported here are archived: reanalysis with corrected sample assignment, receptor-output correlation, offline enrichment, reference-gene audit, external dataset quantification and paired analysis, and the salmon cross-check. Two scripts that generated tables circulated with earlier versions of this work are not archived; every value derived from them has been regenerated with archived code.

References

1. Liu Y, Nishiura M, Fujii M, Sandhu S, Yawaka Y, Yamazaki Y, Hasebe A, Iimura T, Kong SW, Lee JW. Selective Pyk2 inhibition enhances bone restoration through SCARA5-mediated bone marrow remodeling in ovariectomized mice. Cell Commun Signal. 2024;22(1):561. doi:10.1186/s12964-024-01945-8.

2. Lee H, Lee YJ, Choi H, Seok JW, Yoon BK, Kim D, Han JY, Lee Y, Kim HJ, Kim JW. SCARA5 plays a critical role in the commitment of mesenchymal stem cells to adipogenesis. Sci Rep. 2017;7(1):14833. doi:10.1038/s41598-017-12512-2.

3. Li JY, Paragas N, Ned RM, Qiu A, Viltard M, Leete T, Drexler IR, Chen X, Sanna-Cherchi S, Mohammed F, Williams D, Lin CS, Schmidt-Ott KM, Andrews NC, Barasch J. Scara5 is a ferritin receptor mediating non-transferrin iron delivery. Dev Cell. 2009;16(1):35-46. doi:10.1016/j.devcel.2008.12.002.

4. Kumlin M, Ungerstedt J, Cai H, Leonard E, Felländer-Tsai L, Qian H. The functional and molecular impact of triamcinolone acetonide on primary

human bone marrow mesenchymal stem cells. Sci Rep. 2023;13(1):21787. doi:10.1038/s41598-023-48448-z.

Figure Legends

Figure 1. Transcriptomic identification of SCARA5 in Pyk2-inhibited hMSCs. GSE266328; human bone marrow MSCs (Lonza) in osteogenic differentiation medium containing ascorbic acid, β-glycerophosphate and dexamethasone, treated with PF-4618433 (50 nM) or DMSO for 4 days; n = 3 per group; genes filtered at ⩾ 10 summed reads (62,754 → 20,603) before DESeq2 median-of-ratios testing. **(A)** Volcano plot, Pyk2 inhibitor versus control, with SCARA5 and ALPL labelled; 236 genes up and 243 down at adjusted $P < 0.05$ with $|\log2FC| > 1$. **(B)** SCARA5 normalised counts across all six libraries (control 1,127–1,145; Pyk2 inhibitor 144–154; log2FC = −2.94, adjusted P = 4.7e-169). **(C)** Top 50 differentially expressed genes by adjusted P value, variance-stabilised and row-scaled; single-dataset heatmap of GSE266328 only. **(D)** GO Biological Process over-representation plotted by direction.

Figure 2. GR engagement of the SCARA5 axis: promoter element. JASPAR GR/NR3C1 position weight matrix scan of the SCARA5 proximal promoter, identifying a candidate glucocorticoid response element. Motif presence is sequence evidence and is not occupancy.

Figure 3. DESeq2-normalised SCARA5 receptor-output programme. Pearson correlations between log2(normalised count + 1) for SCARA5 and each curated module member, computed on the prefiltered GSE266328 matrix; with n = 6, $p < 0.05$ corresponds to $|r| > 0.811$. **(A)** Module-level summary plotting mean |r| and directional mean r side by side (ferritin/iron mean |r| = 0.909, directional mean = +0.393, 8 of 10 members significant). **(B)** Per-gene correlation with SCARA5, grouped by module. **(C)** Variance-stabilised, row-scaled heatmap of all detectable signature genes with module annotation. **(D)** Effect size against co-expression (log2 fold change versus Pearson r with SCARA5).

Figures

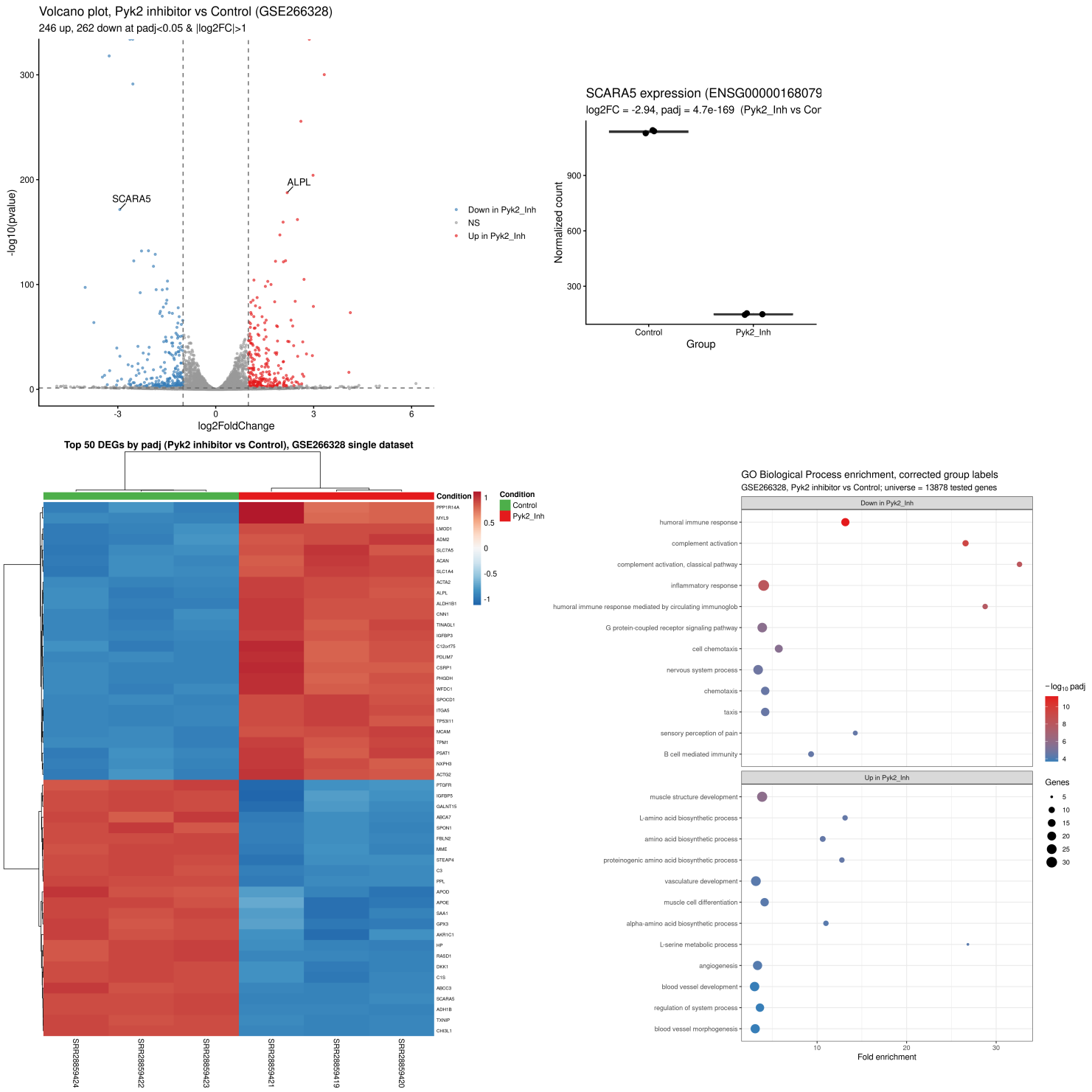


Figure 1

Transcriptomic identification of SCARA5 in Pyk2-inhibited hMSCs. GSE266328; human bone marrow MSCs (Lonza) in osteogenic differentiation medium containing ascorbic acid, β-glycerophosphate and dexamethasone, treated with PF-4618433 (50 nM) or DMSO for 4 days; n = 3 per group; genes filtered at ≥ 10 summed reads (62,754 → 20,603) before DESeq2 median-of-ratios testing. (A) Volcano plot, Pyk2

inhibitor versus control, with SCARA5 and ALPL labelled; 236 genes up and 243 down at adjusted P < 0.05 with |log2FC| > 1. (B) SCARA5 normalised counts across all six libraries (control 1,127–1,145; Pyk2 inhibitor 144–154; log2FC = −2.94, adjusted P = 4.7e-169). (C) Top 50 differentially expressed genes by adjusted P value, variance-stabilised and row-scaled; single-dataset heatmap of GSE266328 only. (D) GO Biological Process over-representation plotted by direction.

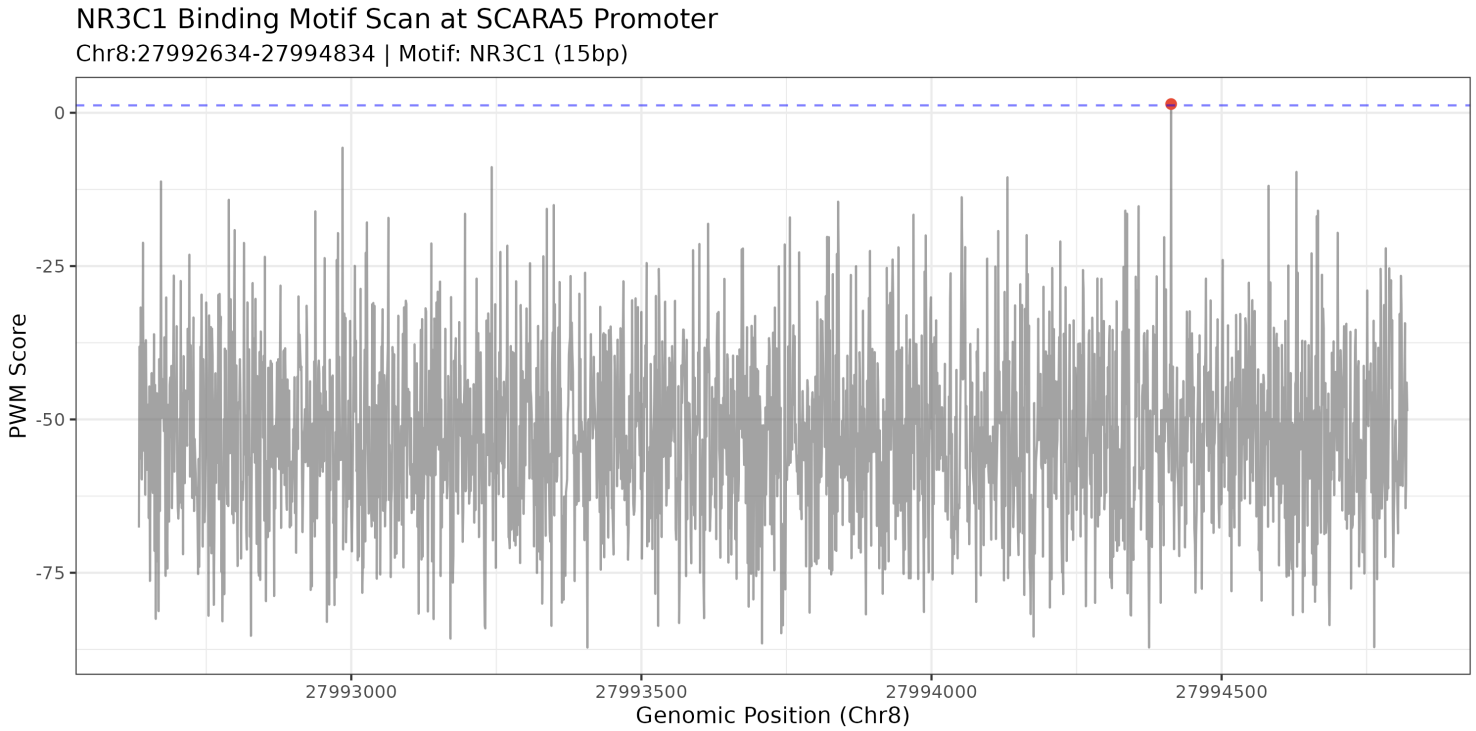


Figure 2

GR engagement of the SCARA5 axis: promoter element. JASPAR GR/NR3C1 position weight matrix scan of the SCARA5 proximal promoter, identifying a candidate glucocorticoid response element. Motif presence is sequence evidence and is not occupancy.

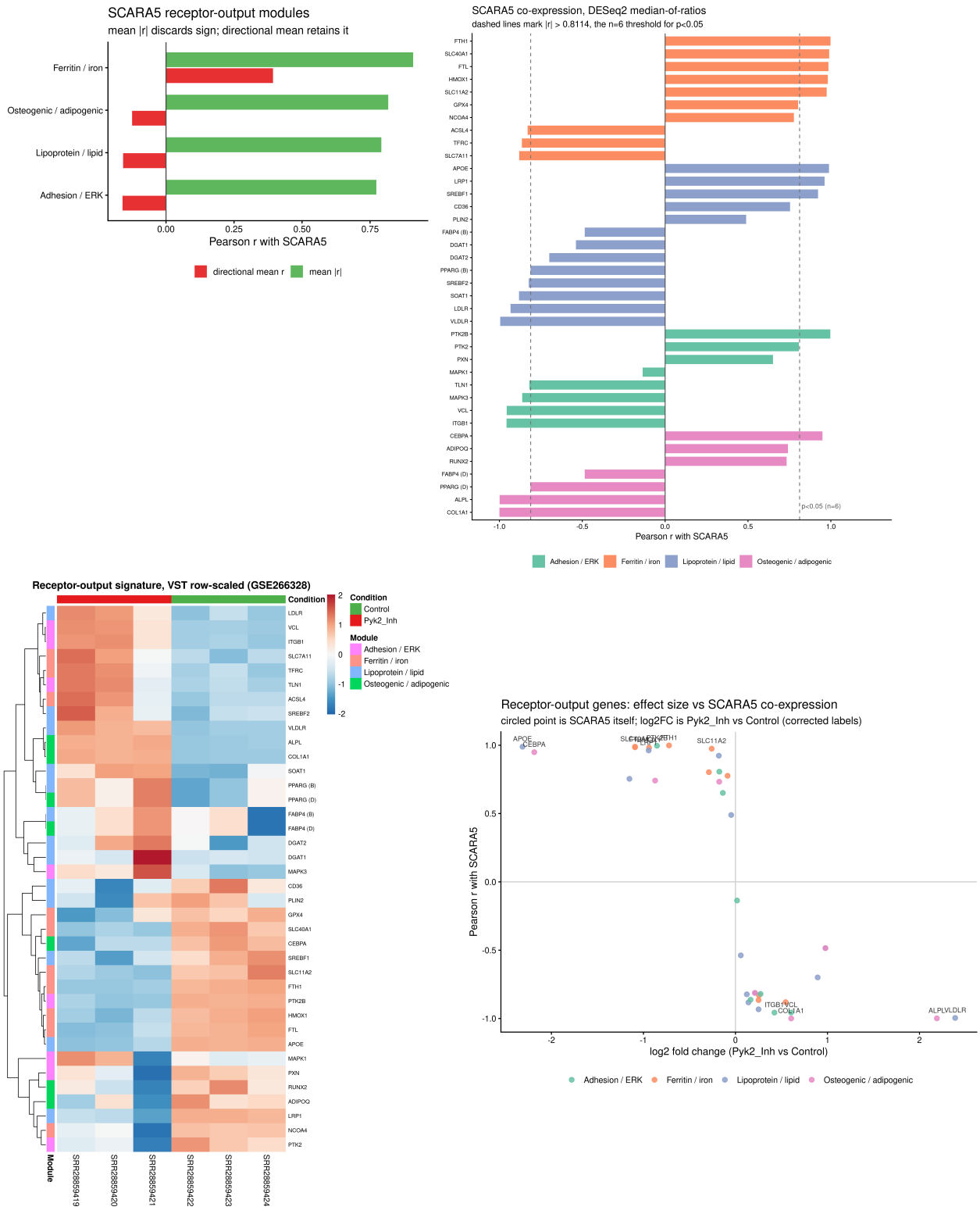


Figure 3

DESeq2-normalised SCARA5 receptor-output programme. Pearson correlations between log2(normalised count + 1) for SCARA5 and each curated module member, computed on the prefiltered GSE266328 matrix; with n = 6, p < 0.05 corresponds to |r| > 0.811. (A) Module-level summary plotting mean |r| and directional mean r side by side (ferritin/iron mean |r| = 0.909, directional mean = +0.393, 8 of 10 members significant). (B) Per-gene correlation with SCARA5, grouped by module. (C) Variance-

stabilised, row-scaled heatmap of all detectable signature genes with module annotation. (D) Effect size against co-expression (log2 fold change versus Pearson r with SCARA5).